9.9 LES STUDY ON THE ENERGY IMBALANCE PROBLEM WITH EDDY COVARIANCE FLUXES FOR UNIFORMLY HEATED CONVECTIVE BOUNDARY LAYERS

Manabu Kanda * , Marcus Oliver Letzel*, Tsutomu Watanabe**, Atsushi Inagaki*, and Siegfried Raasch***
* Tokyo Institute of Technology, Tokyo, Japan
** Forestry and Forest Research Institute, Tsukuba, Japan
*** University of Hannover, Hannover, Germany

1. INTRODUCTION

Accumulation of data in a number of field observation campaigns reveals that the sensible and latent heat fluxes estimated using Eddy Correlation (hereafter EC) method often produce imbalances, in many cases systematic underestimates, of surface energy closure (for example, Twine et al., 2000). Sensor errors related to alignment, response characteristic and flow distortion are possible but not enough to explain such systematic errors of flux estimates. Katul et al. (1999) demonstrated experimentally using seven towers that the spatial variability of fluxes was significant (more than 15 %) even over a homogeneous forest.

The objective of this paper is to investigate the spatial variability of a single point turbulent flux and the mechanism of energy imbalance for homogeneous atmospheric convective boundary layers as a best-case scenario completely free from sensor errors and uncertainties of field conditions. This is done using Large Eddy Simulations (LES) for the daytime atmospheric boundary layer heated uniformly over a flat surface with no synoptic vertical motion but with various horizontal winds. The imbalance intensity is defined as the deviation of local turbulent heat flux from the horizontally averaged one.

2. THEORETICAL BACKGROUND

2.1 Representative Heat Flux

The assumptions related to the present analysis are as follows; (1) no synoptic (large scale) vertical motion in the whole domain, (2) the ground surface is flat and homogeneous, and (3) constant heat flux is supplied from the ground surface. A vertical heat flux of a point distant from the ground surface can be expressed by,

$$F = wT \quad (1),$$

where w and T are vertical velocity component (ms^{-1}) and potential temperature (K), respectively. Decomposing w and T into time average and fluctuation components, and Reynolds-averaging Eq.(1) over time, then

$$\overline{F} = \overline{w}\,\overline{T} + \overline{w'T'} \quad (2),$$

where overbar ($\overline{\ }$) and superscript ' represent time averaged value and fluctuation term, respectively.

The second term on the right hand side in Eq.(2) represents the turbulent correlation that is equivalent to the heat flux estimated from the EC method. The first term on the right hand side in Eq.(2) represents the local mean flow effect that is numerically much larger than the turbulent correlation term and locally meaningless. Horizontally averaging Eq.(2) , we find the 'representative heat flux' at the height

$$[\overline{F}] = [\overline{w}\,\overline{T}] + [\overline{w'T'}] \quad (3)$$

It is important to note that even under the assumption of no synoptic vertical wind the first term in Eq.(3) does not vanish. This means that the conventional turbulent heat flux based on single point measurements cannot produce the proper representative heat flux without the consideration of local mean flow effect, even if a number of point measurements are done for the horizontal averaging. The first term of Eq.(3) can account for the systematic error of the heat flux on the basis of point measurements, but the direct estimation of this term is almost impossible in the field. In the following chapters, the influence of this term will be discussed numerically. The representative heat flux is dependent on the height, and the heat balance between the ground surface and the height can be expressed by,

$$F_g - [\overline{F}] = \int_{z_0}^{z} \overline{\frac{\partial [T]}{\partial t}} dz \quad . \quad (4)$$

2.2 Definition of Imbalance

In this study, the normalized imbalance is defined as the deviation of turbulent heat flux at a local point from the representative heat flux,

$$ib = (\overline{w'T'} - [\overline{F}]) / [\overline{F}] \quad (5).$$

Horizontal averaging of Eq.(5) with consideration of Eq.(3) leads to,

$$[ib] = ([\overline{w}\,\overline{T}]) / [\overline{F}] \quad (6).$$

Eq.(6) means that the horizontal averaged imbalance ratio is directly related to the local mean flow effect. Thus, the systematic error of the EC method is theoretically inevitable as shown by Eqs.(5) and (6), as far as a time series of data at a local point is used for the flux estimation.

* Corresponding author address: Manabu Kanda, Tokyo Institute of Technology, Dept. of International Development Engineering, Meguro-ku, O-okayama, 2-12-1 Tokyo, 152-8552 JAPAN; e-mail: kanda@fluid.cv.titech.ac.jp

3. EXPERIMENTAL DESIGN

PALM (PArallelized Large eddy simulation Model) developed by Raasch and Schröter (2001) has been used. Numerical experiments are designed for typical daytime atmospheric boundary layers with a flat and homogeneous surface. A temporally and spatially constant heat flux of 0.1 (ms^{-1}) is supplied from the ground surface as the thermal forcing. Lateral boundaries are periodic. Rayleigh damping is used to absorb gravity waves in the inversion layer. There exists no synoptic large scale descending/ascending motion. Experiments have been performed with four horizontal wind conditions; 0,1,2 and 4 (ms^{-1}). Relatively calm conditions are chosen, since strong wind conditions over 5 (ms^{-1}) could give rise to problems of LES accuracy (Glendening and Haack, 2001). Three different computational domains are used in order to investigate the influence of computational domain size and resolution (Table1). The summary of all experimental conditions and results is shown in Table2. All computational grid points at a specified height are assumed as virtual observation points and are being used for the analysis of horizontal variability of imbalance. In the numerical analysis, the turbulent correlation term is evaluated as the sum of computed Grid Scale (GS) and Sub-Grid Scale (SGS) components. The contribution of SGS heat flux is insensitive to the computational conditions in the range of the present study and less than 5 % of the total heat flux.

Table 1 Computational Domain

	Size (x-y-z) (km)	Dx (m)	Grid number	DT (sec)
D1	8x8x2.8	50	160x160x50	0.4
D2	8x8x3.2	25	320x320x98	0.25
D3	16x16x2.8	50	320x320x50	0.4

Di: ID number of the domain, DT: time increment
Dx: horizontal grid spacing

Table 2 Summary of computational results

Ei	U_g (ms^{-1})	Grids	T_a (hr)	Z_a (m)	$[ib]$ (%)	σ_{ib} (%)
E1	0	D1	1 3	100 100	22.4 9.6	46.1 60.1
E2	1	D1	1	100	9.6	33.6
E3	2	D1	1	100	3.9	24.4
E4	4	D1	1	100	2.6	18.0
E5	0	D2	1 1 1 1	50 75 100 150	13.8 18.6 22.4 26.6	29.4 37.8 46.1 51.3
E6	0	D3	1	100	22.4	46.1

U_g: horizontal wind, T_a: averaging time, Z_a: height investigated, σ_{ib} : standard deviation of ib ,Ei: ID number of the numerical experiment

4. RESULTS

4.1 Effect of Averaging Time

Fig.1 shows the probability functions of normalized imbalance for different averaging time. The probability function is formulated by

$$p(x) = \frac{N(x)}{N_t dx} \text{ and } \int_{-\infty}^{\infty} p(x)dx = 1 \qquad (7)$$

where x is the normalized imbalance defined by eq.(3), N_t is the total number of grid points for the analyzed plane and $N(x)$ is the number of grid points where imbalances between $x-1/2dx$ and $x+1/2dx$ exist. The probability function for imbalance averaged over 1hr clearly shows a negative bias and the scatter is as large as 46 (%) as shown in Table 2. This strongly corresponds to turbulent organized structures (TOS). These thermally induced structures, so called "spoke like pattern," appear in the plane (Fig.2) and these actually cause the local mean flow term in Eq.(2). Even after 3hrs averaging TOS still remains, although the vertical velocity is smaller and the structure is more ambiguous. It is interesting that the horizontally averaged imbalance averaged over 3hrs becomes smaller but the scatter even larger. This is because the long time averaging includes lower frequency trends corresponding to temporal behavior of TOS. Fig.3 shows 1hr averaged vertical velocities at different time stages. Actually, TOS is slowly moving and not stationary.

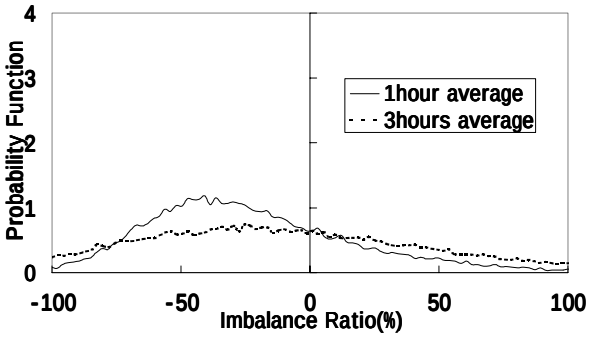

Fig.1 probability functions of imbalance for E1

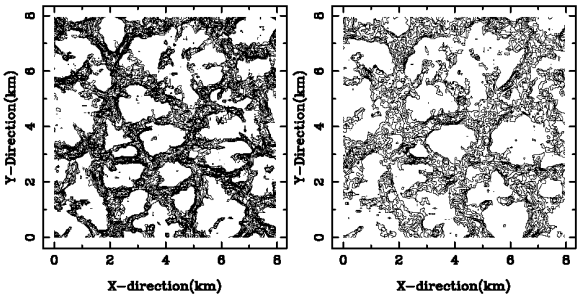

Fig.2 Temporally averaged vertical velocity for E1 left (1hr averaging),right (3hrs averaging) Contour interval 0.1(ms^{-1})

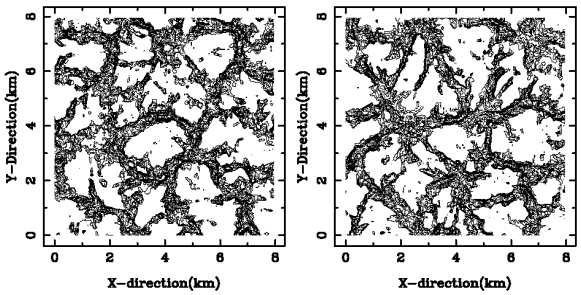

Fig.3 1hr averaged vertical velocity at different times
Left: 3 to 4 hrs after simulation start
Right: 4 to 5 hrs after simulation start
Contour interval is 0.1(ms^{-1}) and results for E1

4.2 Effect of Horizontal Wind

Fig.4 clearly demonstrated that the deviation of flux estimates significantly depends on horizontal wind. Under light or zero wind conditions, the scatter of imbalances is larger and the average of the probability function is more negative. Horizontal averages of eddy covariance imbalances are systematically negative and drastically decrease in accordance with horizontal winds. Standard deviations of imbalances can be as large as 18% of horizontally averaged flux even in case of 4 ms^{-1} (Table2). This value is roughly consistent with the results by Katul et al.(1999) in which more than 15 % spatial variability of flux estimates was observed over a homogeneous forest.

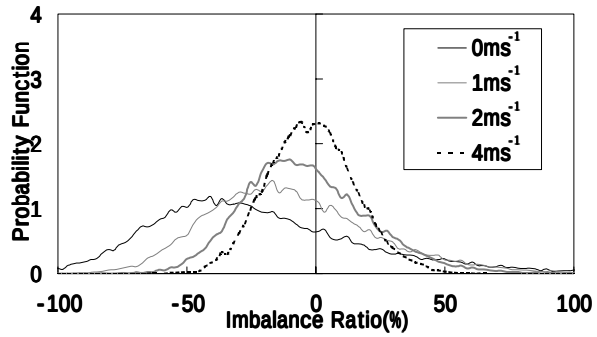

Fig.4 Probability functions of imbalance under different horizontal wind conditions

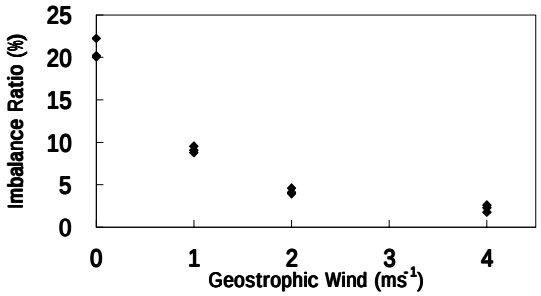

Fig.5 Horizontal winds versus horizontally averaged imbalance for E1,E2,E3 and E4

The “spoke like pattern” of TOS under calm condition is changing to longitudinal vortex when the horizontal wind increases. Roll vortices are more likely aligned with the wind directions and vertical wind velocities are weaker. Such a relationship between TOS pattern and horizontal wind velocity has been investigated by many researches. Especially, the mechanism of roll vortices observed in oceans has been vigorously studied. The strong dependency of imbalance on the horizontal wind velocity as shown in Figs.4 and 5 is closely related to these TOS characteristics. The dependency of imbalance on geostrophic wind has also been reported by many field observations (for example, Mahrt, 1998).

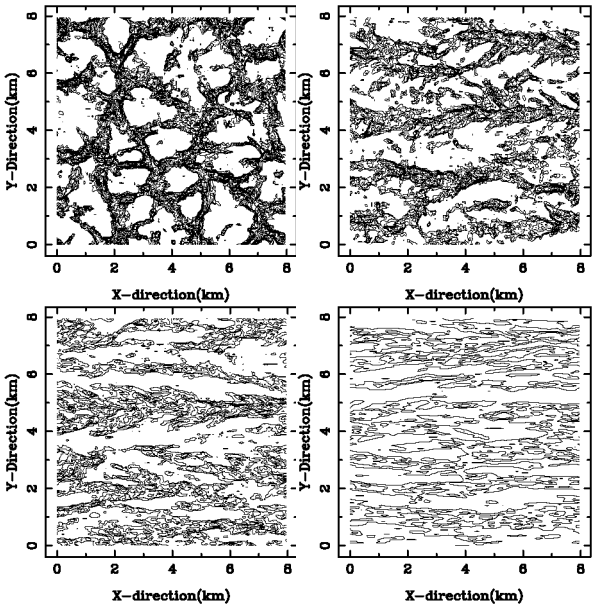

Fig.6 1hr-averaged vertical velocity map (z=100m)
Upper left (U_g=0ms^{-1}),right (U_g=1ms^{-1})
Lower left (U_g=2ms^{-1}),right (U_g=4ms^{-1})
Contour interval 0.1(ms^{-1})

4.3 Effect of Domain Size and Resolution

The influence of domain size and spatial resolution on TOS and resulting imbalance statistics should be investigated, because finer grid could resolve the updraft regions of thermal plumes more sharply and larger domain size might create larger organized structures. Comparison of the results for E1,E5 and E6, however, demonstrates no influence of both factors on imbalance statistics in the range of the present experiments (Table2). TOS patterns simulated in big and small computational domains show also no essential difference (Fig.7). Over the oceans or continents, however, very large TOS with aspect ratio as much as 20 to 40 are often observed (for example, Miura,1980). The mechanism of these large TOS has not been made clear yet. Concerning to this issue, further LES study using much larger computational domain size should be needed.

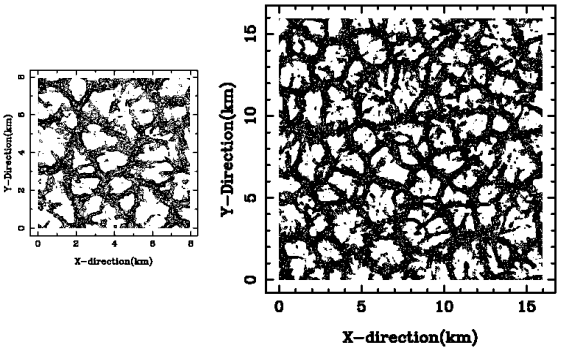

Fig.7 1hr averaged vertical velocity for different computational domains (z=100m).
Left: small domain of D1
Right: large domain of D3

4.4 Effect of Height

Fig.8 shows the probability functions of imbalance for different heights. Higher elevation gives larger imbalance and larger scatter. At lower level, vertical velocity becomes weaker and the edges of thermal lines become more ambiguous due to small scale turbulences, although the TOS at different heights do resemble and correlate each other well (Fig.9).

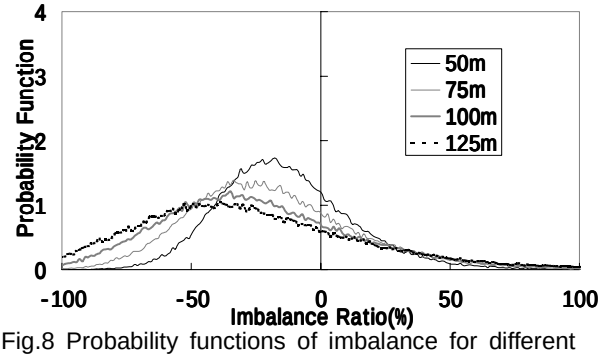

Fig.8 Probability functions of imbalance for different heights (results for E5)

5. CONCLUSION

The spatial variability of a single point turbulent flux and mechanism of energy imbalance for homogeneous atmospheric convective layers are investigated using Large Eddy Simulation. Consequently, the following results are obtained;

(1) Underestimation of EC fluxes is mechanically related to turbulent organized structures that cause local mean velocity contributions additional to turbulent correlation fluxes.
(2) Stronger winds produce smaller imbalance and variability of flux, which agrees with previous field measurements.
(3) Longer averaging times reduce area averaged imbalance but increase flux variability.
(4) At higher elevation both imbalance and flux variability are large.

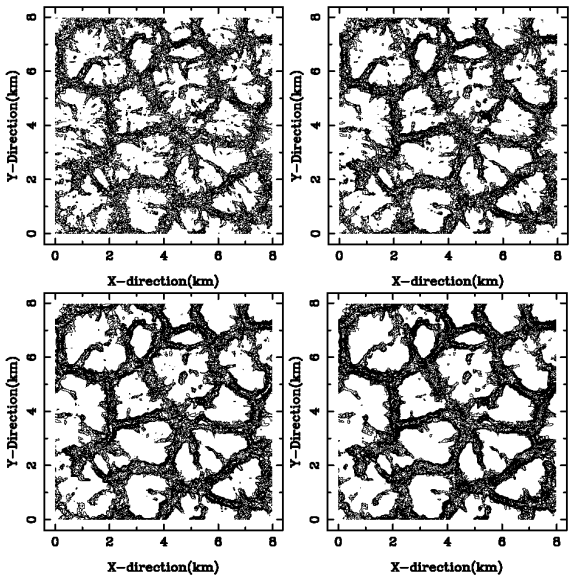

Fig.9 1hr-averaged vertical velocity map for E5
Upper left (z=50 m),upper right (z=75m)
Lower left (z=100m),lower right (z=125m)
Contour interval 0.1(ms^{-1})

REFERENCES

Glendening, J.W. and Haack, T., 2001: Influence of advection differencing error upon large-eddy simulation accuracy, Boundary-Layer Meteorol., **98**, 127-153.

Katul, G., Hsieh, C., Bowling, D., Clark, K., Shurpali, N., Turnipseed, A., Albertson, J., Tu, K., Hollinger, D., Evans, B., Offerle, B., Anderson, D., Ellsworth, D., Vogel, C., Oren, R., 1999: Spatial variability of turbulent fluxes in the roughness sublayer of an even-aged pine forest, Boundary-Layer Meteorol., **93**, 1-28.

Mahrt, L. ,1998: Flux sampling errors for aircraft and towers, J. Atmos. Ocean. Tech., **15**, 416-429.

Miura, Y., 1986: Aspect ratios of longitudinal rolls and convection cells observed during cold air outbreaks, J. Atmos. Sci., **43**, 26-39.

Raasch, S. and Schröter, M., 2001 : PALM - A large-eddy simulation model performing on massively parallel computers. Meteorol. Z., **10**, 363-372. (see also P3.13 in this preprint volume)

Twine, T.E., Kustas, W.P., Norman, J.M., Cook, D.R., Houser, P.R., Meyers, T.P., Prueger, J.H., Starks, P.J., Wesley, M.L., 2000: Correcting eddy covariance flux underestimates over a grassland, Agric. For. Meteorol., **103**, 279-300.